ISSN 1392–1320 MATERIALS SCIENCE (MEDŽIAGOTYRA). Vol. 20, No. 1. 2014

Silicone Rubber and Microcrystalline Cellulose Composites with Antimicrobial Properties

Virginija JANKAUSKAITĖ [1]*, Bekžan ABZALBEKULY [2], Aistė LISAUSKAITĖ [1], Igoris PROCYČEVAS [1, 3], Eglė FATARAITĖ [3, 4], Astra VITKAUSKIENĖ [5], Urynbassar JANAKHMETOV [2]

[1] *Research Centre for Plastic and Leather Products, Faculty of Mechanical Engineering and Design, Kaunas University of Technology, Studentų str. 56, LT-51424 Kaunas, Lithuania*
[2] *Department of Textile Products Technology, Institute of Technology and Information Systems, M. Kh. Dulaty Taraz State University, Tolei bi str. 60, 080000 Taraz, Kazakhstan*
[3] *Institute of Materials Science, Kaunas University of Technology, Savanorių aveniu 271, LT-313432 Kaunas, Lithuania*
[4] *Department of Materials Engineering, Kaunas University of Technology, Studentų str. 56, LT-51424 Kaunas, Lithuania*
[5] *Lithuanian University of Health Science, Faculty of Medicine, Eivenių str. 2, LT-50009 Kaunas, Lithuania*

crossref http://dx.doi.org/10.5755/j01.ms.20.1.4397

Received 17 May 2013; accepted 29 September 2013

The goal of this study was to create polydimethylsiloxane (PDMS) and microcrystalline cellulose (MCC) composites with high mechanical properties and antimicrobial activity. Vinyl-terminated PDMS was mixed with bifunctional filler, which combines MCC stiffness and antimicrobial properties of silver nanoparticles. To provide antimicrobial properties the silver nanoparticles *in situ* were synthesized by chemical reduction method in MCC aqueous suspension. Silver nanoparticles (AgNPs) concentration deposited on MCC particles surface was varied. The morphology, antimicrobial activity and mechanical properties of PDMS/MCC composites and their components have been investigated. It was shown that the combination of MCC/AgNPs as a filler and PDMS as matrix advantages bring multifunctional properties to polymer matrix composite.

Keywords: polydimethylsiloxane, microcrystalline cellulose, silver nanoparticles, structure, antibacterial properties, mechanical properties.

1. INTRODUCTION

Silicones due to their biocompatibility and biodurability have found widespread application in orthopaedic and medicine fields [1 – 3]. Silicones are synthetic polymers whose skeletal backbone is made up of silicon-oxygen bonds [1, 3]. The basic repeating unit of a linear polysiloxane molecule has the structure –(RR'SiO)$_n$–. The most common member of the siloxane family is polydimethylsiloxane (PDMS), when both R and R' are methyl groups. PDMS has found many applications due to their unique properties, which arise mainly from the nature of the siloxane bond (Si–O) [3 – 6]. These properties include extremely low glass transition temperature (–123 °C), low surface energy, good insulating properties, high permeability to gases and very good chemical and thermal stability [4]. However, PDMS is characterized by poor mechanical properties. The reinforcing fillers are added to overcome this problem. Most studies have been focused on the use of synthetic and inorganic fillers such as fumed or precipitated silica, carbon black, boron nitride, to improve silicones mechanical behaviour [3, 7 – 10]. Much less researchers have been turn on bio-based materials [11, 12].

Interest in cellulose-reinforced composites and nanocomposites has increased in recent years [13 – 15]. Cellulose is a linear-chain carbohydrate polymer characterized by a high molecular weight homopolymer of β-1,4-linked anhydro-D-glucose units. Cellulose characteristics and chemical properties are closely associated with its molecular structure [16, 17]. Amorphous and crystalline regions are present within solid-state cellulose. Amorphous regions can be easily hydrolyzed by acid, while crystalline regions have a higher acid resistance [17]. Using acid treatment of cellular cellulose microcrystalline cellulose (MCC) can be produced. This material is a very promising reinforcement for polymers [18 – 21]. MCC particles are inherently fairly stiff and act as reinforcement for various polymer matrixes including PDMS as show our investigations [22].

However, monofunctional filler often can only improve a single property of polymer. Therefore, to prepare polymer materials with enhanced properties, compositions of various fillers or nanofillers can be mixed with polymer matrix. Inorganic nanoparticles (i. e. metallic) are important types of nanofillers that have been successfully used for the functionalization of polymer materials [23, 24]. The synthesis of metallic nanoparticles is generally carried out by reducing metal salts in the presence of surfactants or polymeric ligands to prevent from particles aggregation [25, 26]. The use of various materials as carriers for metallic nanoparticles and formation of organic/inorganic hybrid nanomaterials at present has been intensively investigated [27, 28]. Cellulose-based particles and metal nanoparticles composites as multifunctional fillers within polymer matrices also are possible [29, 30].

*Corresponding author. Tel.:+370-37-300207, fax: +370-37-353989, E-mail address: *virginija.jankauskaite@ktu.lt* (V. Jankauskaitė)

Silver (Ag) as a nonspecific biocidal agent is able to act strongly against broad spectrum of bacterial and fungal species [31]. Although the antibacterial properties of silver are not fully understood, several researchers have demonstrated that Ag nanoparticles attach to the bacterial cell membranes modify its permeability and disturb respiratory function [32]. The tiniest Ag nanoparticles were also shown to penetrate bacterial cells and probably bind DNA [31, 33, 34]. However, latest investigations show that the antibacterial properties of Ag nanoparticles are the result of the release of Ag^+ ions and are not caused by the nanoparticles themselves [35]. Alvarez P. J. J. et al. suggest that the insoluble AgNPs do not kill bacteria cell by direct contact, but the soluble ions, activated by oxidation in the vicinity of bacteria, kill microbes. On the other words, the key determinant of Ag nanoparticles toxicity are not size, shape, and coating of the particles, but the amount of Ag^+ ions that are released. Thus, according to these researchers the antibacterial mechanism of silver nanoparticles should be focused on the mas-transfer process and controlled release mechanism [35].

This study focuses on the possibility to improve polydimethylsiloxane properties using bifunctional filler that combines strengthening capability of microcrystalline cellulose with antimicrobial properties of silver nanoparticles.

2. EXPERIMENTAL

2.1. Materials

Silicone. Vinyl-terminated PDMS, Endeavour T-2516 (Endeavour Enterprise Co, Taiwan), applied for orthopaedic applications (i. e. knee pads, shoes pads inserts, etc.) was used for investigations. This PDMS is two-part (A:B) room temperature vulcanizing rubber, which cross-linking is catalysed by platinum complex. Platinum complex participate in a reaction between a hydride functional siloxane polymer and a vinyl functional siloxane polymer resulting in an ethyl bridge between the two polymers as is pictured in Scheme 1 [2, 4]. Main properties of PDMS rubber to be used are listed in Table 1.

Table 1. Main properties of used PDMS

Property	Units	Value
Viscosity A : B = 1 : 1 (25 ºC)	Pa s	3.5
Specific gravity	–	1.02
Hardness	Shore A	10
Thermal conductivity	W/(m·K)	0.2
Dielectric strength	kV/mm	27
Dielectric constant (25 ºC, 100 kHz)	–	4.5
Volume resistivity	Ω·m	$2.2 \cdot 10^{-16}$

Microcrystalline cellulose. For investigations applied MCC (Sigma Aldrich) is purified, partially depolymerized cellulose prepared by mineral acids treating of α-cellulose, obtained as a pulp from fibrous plant material. MCC particles size varies in the range of 20 μm (Table 2).

Chemicals. Silver nitrate ($AgNO_3$; M = 169.87 g/mol), sodium borohydride ($NaBH_4$; M = 37.83 g/mol), and polyvinylpyrrolidone (PVP, $(C_6H_9NO)_x$; $M \approx 24000$ g/mol) were bought from Sigma Aldrich.

Table 2. Main properties of MCC

Property	Units	Value
Appearance	–	white powder
Loss on drying	%	<5.0
pH	–	5.5 – 7.0
Particle size distribution d50	μm	18 – 22
Bulk density (25 ºC)	g/mL	0.5

2.2. Sample preparation

Silver nanoparticles synthesis. Silver nanoparticles (AgNPs) were synthesized using one of the most popular chemical reduction method. The starting point of the synthesis was the production of a silver nitrate ($AgNO_3$) solution. When silver nitrate is dissolved it splits into a positive silver ion (Ag^+) and a negative nitrate ion (NO_3^-). In order to turn the silver ions into solid silver, the ions have to be reduced by receiving an electron from a donator. Ice-cold sodium borohydride $NaBH_4$ was used to reduce precursor silver nitrate $AgNO_3$. The silver nitrate reduction reaction can be written as:

$$AgNO_3 + NaBH_4 \rightarrow Ag + 0.5H_2 + 0.5B_2H_6 + NaNO_3 . \quad (1)$$

In this study to prepare the microcrystalline cellulose/silver (MCC/AgNPs) nanocomposites *in situ* reduction of $AgNO_3$ in MCC aqueous suspension was applied. Initially 200 mg of MCC 1 h was dispersed in 100 ml deionized water. The suspension was stirred vigorously on a magnetic stir plate. PVP (100 mg) as colloidal stabilizer and $AgNO_3$ (1×10^{-2} M) were added dropwise (about 1 drop/sec) to the MCC suspension (100 g, 2 %). After stirring for 30 min $NaBH_4$ (1×10^{-2} M) was added. The suspension was reduced and changed from colourless to yellow. After stirring for another 1 h, the MCC/AgNPs nanocomposite was filtrated in vacuum, several times washed with deionized water and acetone and, finally, dried at 60 ºC for 4 h.

Table 3. MCC/AgNPs nanocomposites characterization

$AgNO_3$ amount in MCC suspension, mL	Code	Ag concentration, wt.%
0	MCC	0
1.0 (without PVP)	MCC / AgNPs-2	0.16
1.0	MCC / AgNPs-3	0.18
3.0	MCC / AgNPs-4	0.21
5.0	MCC / AgNPs-5	0.32
10.0	MCC / AgNPs-6	0.51

To prepare composites with different AgNPs content, the aqueous $AgNO_3$ content in MCC suspension (100 ml, 2 %) was varied between 1 mL and 10 mL, keeping the same concentration of $NaBH_4$. Increase of the $AgNO_3$ concentration darkened suspension colour from yellow to brown. The prepared MCC/AgNPs nanocomposites are listed in Table 3.

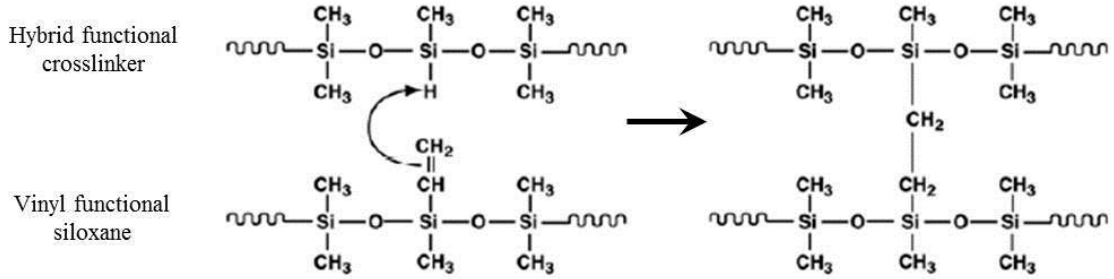

Scheme 1. PDMS addition curing mechanism catalysed by platinum complex [2]

A Perkin Elmer 403 flame atomic absorption spectrometer, equipped with appropriate hallow cathode lamp and air-acetylene burner, was used for the determination of silver concentration in MCC/AgNPs nanocomposites. The instrumental parameters were as follows: wavelength of 328.1 nm; lamp current of 5 mA; band pass of 0.5 nm [36].

Silicone specimens preparation. RTV silicone rubber (PDMS) specimens were produced using the following processing route: (i) mixing the MCC with vinyl functional silicone in appropriate amount and sonifying for 10 min, (ii) blending two liquid components, i. e. vinyl functional siloxane and hybrid functional crosslinker with A : B = 1 : 1 ratio; (iii) putting the uncured mixture under vacuum for 60 min in order to eliminate undesirable entrapped bubbles, (iv) pouring the liquid mixture in moulds, (v) putting moulds inside the oven at 70 ºC for 25 min to cure the silicone.

Dog-bone test pieces were used for uniaxial tensile tests with gage area of (25 ±1) mm × (4 ±0.1) mm and thickness of (4 ± 1) mm. The specimens were moulded in the polyethylene terephthalate multicavity mould produced by compression moulding. For compression testing silicone shoe pad inserts moulded in special shaped epoxy mould were applied.

2.3. Characterization

Microscopy. The filler and composites structures were studied from images obtained by SEM FEI Quanta 200 FEG (FEI, USA). The samples were examined in low vacuum mode operating at 20.0 kV using an LDF detector. The content of AgNPs and chemical analysis of nanocomposites were performed by the energy dispersive spectroscopy SEM/EDS technique with a Brucker XFlash 4030 detector (accelerating voltage 10 kV, distance between the bottom of the objective lens and the object 10 mm).

Polarized light microscopy examinations using B-600 MET (Optika S.R.L., Italy) with a capture camera were carried out on the cast samples. The magnification of ×750 was used to examine the samples.

Wettability. Contact angle measurements were performed at ambient temperature by sessile drop method. A drop of deionized water (*ca.* 5 µL) was deposited onto silicone surface. After 10 s of dropping the drop was recorded with PC-connected digital camera. Contact angle was measured using method based on B-spline snakes (active contours) [37, 38]. This method offers the best trade-off between the use of the general drop shape to guide detection of the drop contour, and the use of an algorithm with local behaviour to compute contact angles with high accuracy [39]. The left and right contact angles of each drop were estimated. At least three measurements were performed to evaluate polymer surface and mean values calculated. The mean standard deviation of the measurements was 1 – 2 degrees.

Antimicrobial investigations. The antimicrobial properties were evaluated against *Staphylococcus aureus* ATCC 25923, Gram-positive bacterium and *Escherichia coli* ATCC 25922, Gram-negative one. The kinetic of bacteria death rate was determined by method that is based on the inoculation of 0.1 ml of Tryptone soy broth (TSB, USA) media containing 3×10^8 cfu/ml from each isolate into sterile tubes. Each tube contained 20 ml of TSB and 10 µg/ml MCC/AgNPs particles. The media were incubated at 37 °C for 0, 1, 3, 7, 10, 15, 30, 45, 60, 120, 180 and 240 min (for tube 1 to 12, respectively) [40, 41]. Using a sterile swab, samples from these tubes were sub-cultured onto Columbia Agar with 5 % of Sheep Blood (Becton Dickinson, USA) plates and incubated at 37 °C for 72 h. Bacterial survival was recorded over a 4 h period.

Mechanical testing. Uniaxial tensile tests were carried out at room temperature using universal testing machine H25KT with load cell of 1 kN (Tinius Olsen, Redhill, England). A cross-head speed of 100 mm/min was used for this study. Measurements were performed at room temperature with the dog-bone test pieces. Five test pieces were tested for each set of samples and the mean values were calculated.

Uniaxial compression tests were carried out using universal testing machine H25KT with load cell of 25 kN (Tinius Olsen, England) at loading speed of 10 mm/min. Measurements were performed with moulded silicone shoe pads inserts at 20 % of compression strain. Compression testing set to be used is shown in Fig. 1. Not less than three test pieces were tested for each set of samples.

Silicone hardness was defined as samples resistance to permanent indentation using Shore A durometer HPSA-M (Albuquerque Industrial, USA) with spring loaded needle-like indenter foot with end diameter of 0.079 mm. The sheet samples of thickness not less than 6.0 mm were used. At least five measurements were performed and mean value calculated.

3. RESULTS AND DISCUSSION

3.1. Morphology

The overview and detailed appearance of the used MCC particles are shown in Fig. 2. As can be seen, MCC is in particulate form and the particles dimensions are in the range of (10 – 20) µm, while aspect ratio varies

between 2 and 4. Usually, as can be seen from SEM images, MCC particles form aggregates (Fig. 2, a). A fairly rough surface is characteristic for MCC particles (Fig. 2, b). It is also possible to see some nanofibrils on the MCC particles surface, which may be evidence that MCC particles are agglomerates of hundreds of individual cellulose nanofibrils.

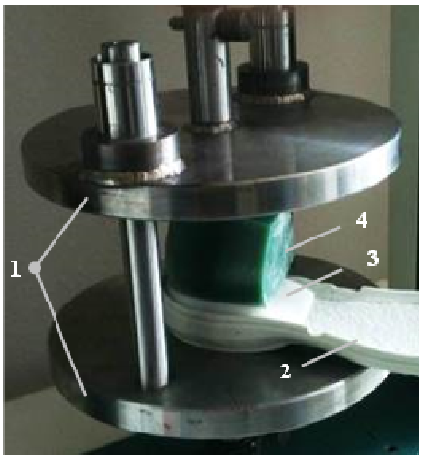

Fig. 1. Compression testing set: 1 – clamps; 2 – outsole; 3 – test piece (shoe pad insert); 4 – punch

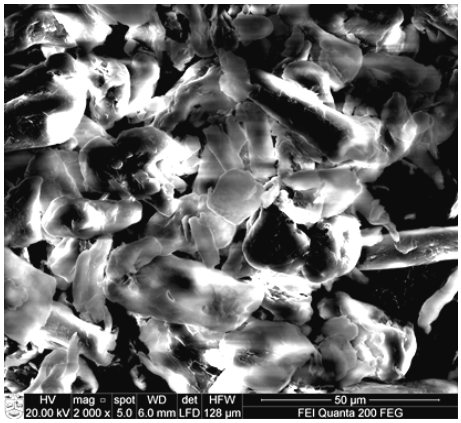

a

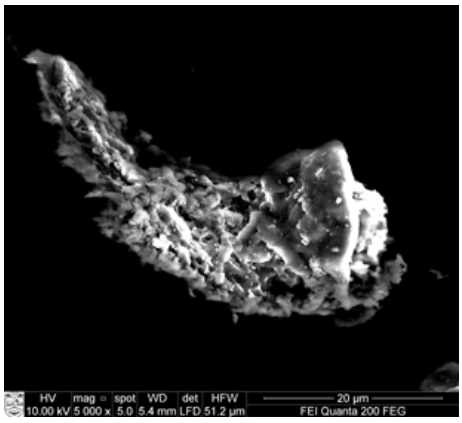

b

Fig. 2. Structure of MCC particles: a – overview; b – particle surface image

SEM image of MCC/AgNPs nanocomposite at silver concentration of 0.5 wt.% is presented in Fig. 3, a. It is evident that AgNPs synthesized on MCC particles surface from the colloidal solution shows silver to be nanosized and agglomerated. Measurements show that the nanoparticles diameter varies in the range of 25 nm – 85 nm.

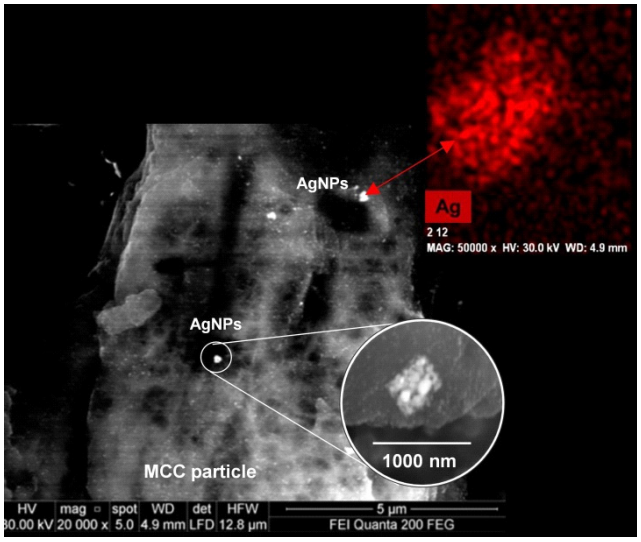

a

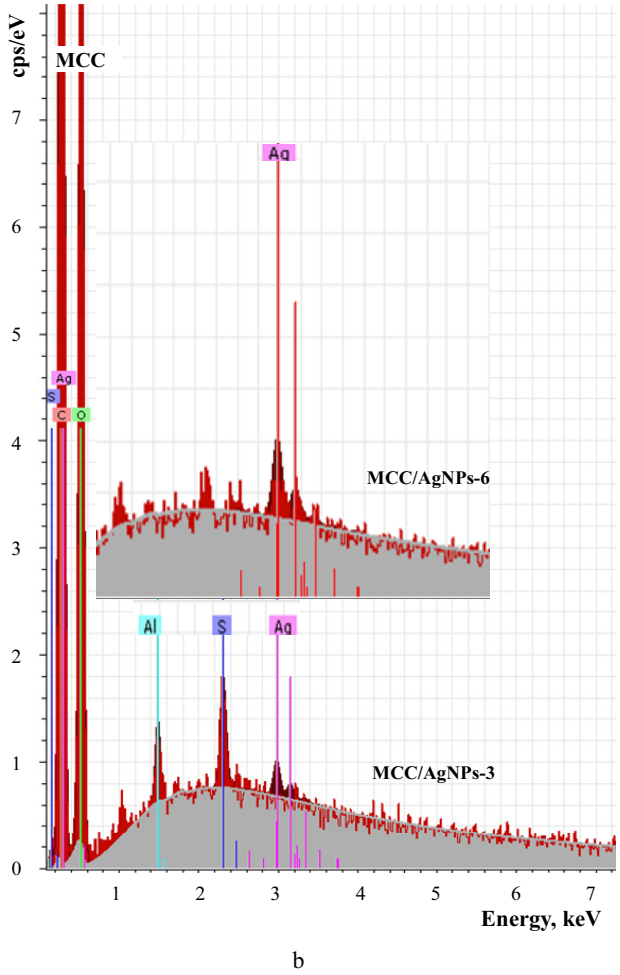

b

Fig. 3. SEM image of MCC/AgNPs nanocomposite (a) and EDS analysis map for Ag (b)

Fig. 3, b, shows EDS spectra of the MCC with deposited AgNPs. The peaks around 0.15 keV and 0.3 keV are related to the binding energy of MCC, while peaks at 1.25 keV and 2.15 keV can be attributed to the binding energy of glass that was used as substrate. The peak around

3.0 keV is related to the silver elements in MCC/AgNPs nanocomposites with different silver concentration. Besides, the increase of AgNPs percentages in MCC after reduction increases the intensity of silver binder energy peak in the EDS spectra.

The fracture surfaces of the PDMS/MCC composites were studied to understand the failure mechanism and possible interaction between components. The fracture surfaces of the composites are given in Fig. 4. Overview of composite surface shows a uniform dispersion of MCC particles in PDMS matrix (Fig. 4, a). At higher filler loading MCC particles form aggregates, but in some cases separation take place during mixing.

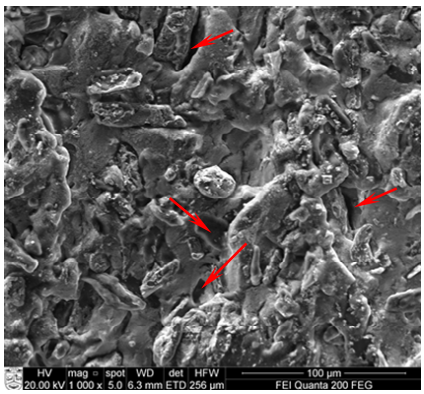

a

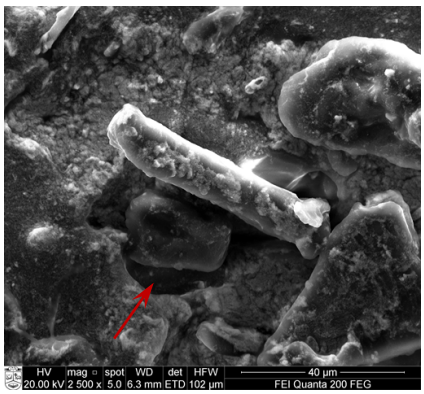

b

Fig. 4. SEM images of PDMS/MCC composites with 5 wt.% (a) and 20 wt.% (b) of filler tensile fractured surface at various magnification: a – 1000×; b – 25000×

As can be seen from Fig. 4, large number of holes is visible in PDMS matrix, where MCC particles were located before fracture. More detailed SEM micrograph Fig. 4, b, shows that there are voids around some MCC particles. Both observations, voids around MCC and holes in the matrix, indicate that there is poor adhesion interaction at the PDMS and MCC interface.

The siloxane films were observed through crossed polarized light (Fig. 5). PDMS composite show birefringence, which is due to the crystalline behaviour of the MCC. It obvious that MCC particles are randomly oriented in the composite film and their dimension are not homogeneous.

MCC due to the hydrophilic nature influences not only composite morphology, but PDMS surface properties also. As can be seen from data, listed in Table 4, addition of MCC influences on the PDMS films wettability behaviour. The unfilled PDMS surface can be characterized as highly hydrophobic (θ = 112º – 113º), but addition of hydrophilic MCC improves surface wettability and decreases contact angle in 9 % – 15 % depending on the filler amount.

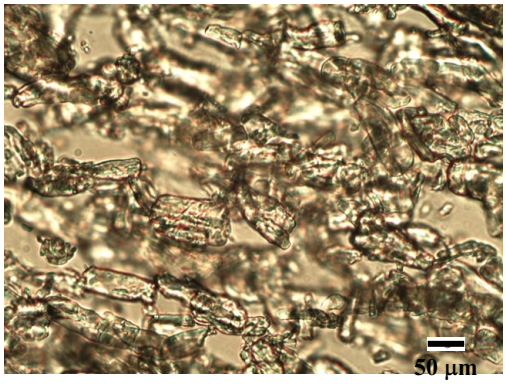

Fig. 5. PDMS/MCC (15 wt.%) composite film observed under crossed polarized optical microscopy (magnification ×750)

Table 4. Dependence of PDMS wettability behaviour upon MCC content

MCC content, wt.%	Contact angle θ, degree:	
	left	right
0	112	113
10	102	102
20	99	98

3.2. Antimicrobial activity

The biocidal action of silver nanoparticles against many species of bacteria is well known and widely used [32, 33, 41 – 43].

Previous our tests performed against Gram-positive bacterium *S. aureus* and gram-negative bacterium *E. coli* using disc diffusion or Kirby-Bauer method [40] containing different concentration of silver did not reveal any changes in antimicrobial activity of MCC/AgNPs nanocomposites. No inhibition zones were observed that did not allow to confirm the diffusion of silver nanoparticles from nanocomposite to culture medium.

However, analysing sterile tubes inoculated with the tested Gram-positive and Gram-negative bacteria it was obtained that MCC/AgNPs inhibit bacteria and fluctuation in antibacterial activity is observed with varying silver content. The presence of nanoparticles at 0.32 % – 0.51 % silver concentration inhibits *S. aureus* bacteria growth by *ca.* 50 % after 1 h of incubation (Fig. 6), while nanocomposites with lower content of silver (0.18 % – 0.2 %) – after 2 h incubation. Some antibacterial activity of MCC/AgNPs nanoparticles is observed to *E. coli* bacteria, also. But in this case the antibacterial activity of nanocomposite is weaker than that to *S. aureus*.

It may be supposed that antimicrobial activity of AgNPs is solely due to the Ag^+ release and even relatively low concentration of silver ions account for the biological response [35].

However, further increase of incubation duration causes bacteria colonies growth and multiplication. It may

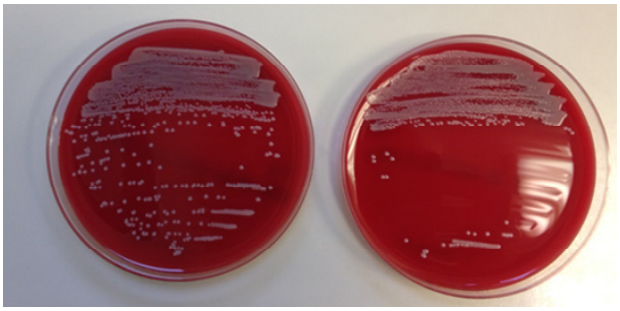

$\tau = 0$ h $\tau = 1$ h

Fig. 6. Appearance of inhibitory zones after MCC/AgNPs nanocomposite contact with *S. aureus* and after incubation 1 h at 37 °C

be supposed that content of AgNPs deposited on the MCC surface is low and shows inconsiderable susceptibility for preventing bacteria growth. Additionally, as show early investigations (Fig. 3, a), AgNPs were observed in aggregates, which demonstrates that prevention from particles aggregation during nanoparticles reduction was unsuccessful. Therefore, AgNPs has only bacteriostatic effect on the bacteria colonies, when bacteria are only inhibited, but not killed. Thus, the modification of MCC surface by oxidation and preparation of carboxylated cellulose, which allow to increase silver concentration on the cellulose particles, is necessary.

3.3. Mechanical properties

The effect of MCC content on the tensile strength, elongation at break and Shore A hardness are shown in Fig. 7.

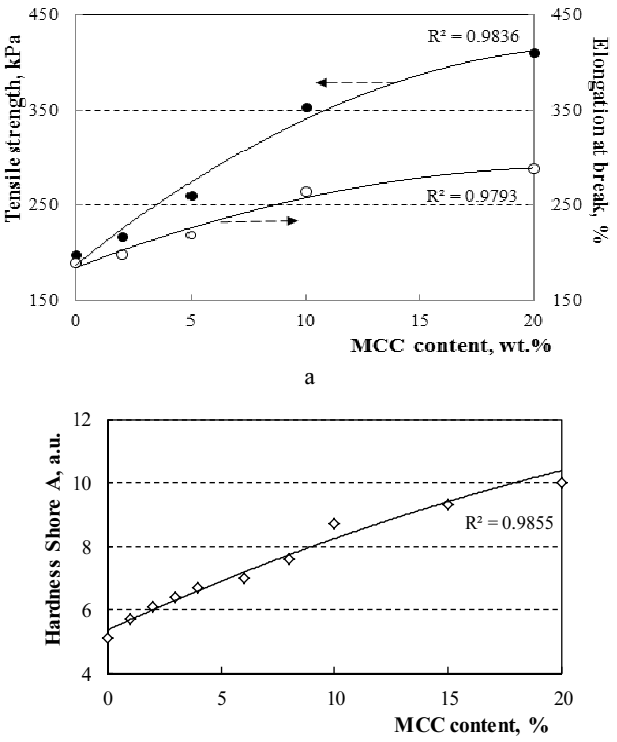

Fig. 7. Dependence of PDMS mechanical properties upon MCC content: a – tensile strength and elongation at break, b – Shore A hardness

The tensile strength of vulcanized PDMS composites increases with the increase of MCC loading PDMS (Fig. 7, a). The composites with 5 wt.% of MCC have tensile strength of 260 kPa, which is in 32 % higher than that of pure PDMS. Addition of higher content of filler yet more strengthen composites. In the case of 20 wt.% MCC the composite strength increases more than twice.

Similar influence of MCC content is observed in the case of elongation at break. As can be seen from Fig. 7, a, PDMS composite with 20 wt.% of MCC shows 1.5-times higher deformation ability than that of unfilled PDMS.

The Shore A hardness also increases almost linearly with the increase of MCC content (Fig. 7, b). The pure PDMS has hardness of 5.1 Shore A, while hardness of the PDMS/MCC 20 wt.% composite increases up to value of 11.4 Shore A units. The improvement in mechanical properties can be attributed to the composites stiffness increase with the loading of stiff MCC particles.

The compression behaviour of PDMS composite at various MCC content was investigated also and knee pads testing results are presented in Figure 8.

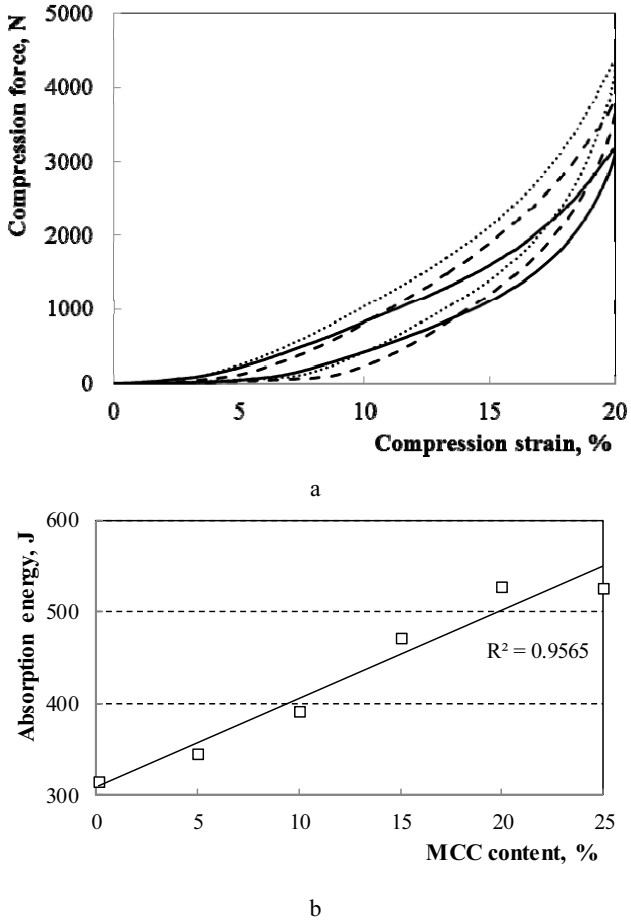

Fig. 8. Dependence of the compression behaviour of PDMS at 20 % deformation upon MCC content: a – compression hysteresis (—— – without MCC; - - - – 15 wt.% of MCC; · · · · – 25 wt.% of MCC); b – absorption energy

It is evident that MCC increases compression resistance of PDMS and degree of changes depends upon filler loading. The compression force and area of the hysteresis loops at 20 % compression strain increase with the increase of MCC content in PDMS matrix (Fig. 8, a).

Such behaviour shows that absorption energy of silicone knee pads also increases. As can be seen from Fig. 8, b, absorption energy changes according to the linear dependence. The mixing of 10 wt.% MCC changes absorption energy from 314 J up to 392 J (increase in 20 %), while addition of 20 wt.% of filler increases pads absorption ability in 40 %. Higher loading of MCC does not cause further increase of the absorption energy.

The investigations reveal that for filling using MCC/AgNPs nanocomposites, with silver concentration of (0.16 – 0.5) wt.%, PDMS matrix mechanical properties have higher values in 3 % – 11 %. It may be supposed that high surface energy AgNPs increase MCC adhesion with PDMS matrix. However, the influence of silver concentration on mechanical behaviour was ambiguous and more searching investigations are necessary. Thus, the combined advantages of MCC/AgNPs as filler and PDMS as matrix bring multifunctional properties.

4. CONCLUSIONS

This study was carried out as an initial step towards the supply antibacterial properties of microcrystalline cellulose (MCC) and uses such nanocomposite as reinforcement of polydimethylsiloxane (PDMS) matrix.

MCC exists as aggregates of nanofibres of cellulose. The voids around some MCC particles demonstrate that there is poor adhesion interaction at the PDMS matrix and MCC particles interface.

Cellulose and silver nanocomposites (MCC/AgNPs) were successfully prepared by *in situ* reduction of silver nitrate in aqueous MCC suspension. Obtained MCC/AgNPs nanocomposites inhibited the growth and multiplication of the Gram-positive *Staphylococcus aureus* and Gram-negative *Escherichia coli* bacteria at initial time of incubation. However, antibacterial activity of such nanocomposite was only bacteriostatic due to the insufficient silver concentration deposited on the MCC particles and silver nanoparticles tendency to the aggregation.

Mechanical properties of the PDMS/MCC composite are superior to compare to those of unfilled polymer, due to the increase of composite stiffness. Deposition of AgNPs on the MCC increases filler particles adhesion interaction with PDMS matrix.

Acknowledgments

This work was funded by the European Social Fund and Republic of Lithuania (project VP1-3.1-ŠMM-10-V-02-013).

REFERENCES

1. **Hron, P.** Hydrophilisation of Silicone Rubber for Medical Applications *Polymer International* 52 (9) 2003: pp. 1531 – 1539.
2. **Colas, A. Curtis, J.** Silicone Biomaterials: History, Chemistry and Medical Applications of Silicones in *Biomaterials Science*, 2nd ed., Ratner B. D., Ed.; Elsevier: London, UK, 2004: pp. 80 – 86; 697 – 707.
3. **Chen, Q., Liang, Sh., Thouas, G. A.** Elastomeric Biomaterials for Tissue Engineering *Progress in Polymer Science* 38 (3 – 4) 2013: pp. 584 – 671.
4. **Andriot M., et al.** Silicones in Industrial Application. Dow Corning Corp., 2009: 106 p.
5. **Mata, A., Fleischman, A. J., Roy, S.** Characterization of Polydimethylsiloxane (PDMS) Properties for Biomedical Micro/Nanosystems *Biomedical Microdevices* 7 (4) 2005: pp. 281 – 293. http://dx.doi.org/10.1007/s10544-005-6070-2
6. **Yi Zhao, Xin Zhang.** Mechanical Properties Evolution of Polydimethylsiloxane During Crosslinking Process *MRS Proceedings* 975 2006: 0975-DD06-07 (doi:10.1557/PROC-975-0975-DD06-07).
7. **Paul, D. R., Mark, J. E.** Fillers for Polysiloxane ("Silicone") Elastomers *Progress in Polymer Science* 35 (7) 2010: pp. 893 – 901. http://dx.doi.org/10.1016/j.progpolymsci.2010.03.004
8. **Nabarun, R., Bhowmick, A. K.** Tailor-Made Fibrous Hydroxyapatite/Polydimethylsiloxane Composites: Insight into the Kinetics of Polymerization in the Presence of Filler and Structure–Property Relationship *Journal of Physical Chemistry C* 116 (50) 2012: pp. 26551 – 26560. http://dx.doi.org/10.1021/jp305373w
9. **Kahraman, M., Nugay, N.** Polydimethylsiloxane Composites Reinforced by Fumed Silica/Mica Hybrid Reinforcers *International Journal of Polymeric Materials and Polymeric Biomaterials* 51(1 – 2) 2002: pp. 151 – 165.
10. **Kong, S. M., Mariatti, M., Busfield, J. J. C.** Effects of Types of Fillers and Filler Loading on the Properties of Silicone Rubber Composites *Journal of Reinforced Plastics and Composites* 30 (13) 2011: pp. 1087 – 1096.
11. **Fernandes, A. G., Pietrini, M., Chielini, E.** Bio-based Polymeric Composites Comprising Wood Flour as Filler *Biomacromolecules* 5 (4) 2004: pp. 1200-5.
12. EP 2511326. Composite Material Comprising Bio-based Filler and Specific Polymer, 2012.
13. **Siro, I., Placket, D.** Microfibrillated Cellulose and New Nanocomposite materials: A Review *Cellulose* 17 (3) 2010: pp. 459 – 494.
14. **Eichhorn, S. J., et al.** Review: Current International Research into Cellulose Nanofibres and Nanocomposites *Journal of Materials Science* 45 (1) 2010: pp. 1 – 33.
15. **Laka, M., Chernyavskaya, S., Shulga, G., Shapovalov, V., Valenkov, A., Tavroginskaya, M.** Use of Cellulose-Containing Fillers in Composites with Polypropylene *Materials Science* (*Medžiagotyra*) 17 (2) 2011: pp. 150 – 154.
16. **Klemm, D., Heublein, B., Fink, H. P., Bohn, A.** Cellulose: Fascinating Biopolymer and Sustainable Raw Material *Angewandte Chemie International Edition* 44 (22) 2006: pp. 3358 – 3393.
17. **Habibi, Y., Lucia, L. A., Rojas, O. J.** Cellulose Nanocrystals: Chemistry, Self-Assembly, and Applications *Chemical Reviews* 110 (6) 2010: pp. 3479 – 3500.
18. **Zugenmaier, P.** Materials of Cellulose Derivatives and Fiber-Reinforced Cellulose–Polypropylene Composites: Characterization and Application *Pure and Applied Chemistry* 78 (10) 2006: pp. 1843 – 1855.
19. **Petersson, L., Oksman, K.** Biopolymer Based Nanocomposites: Comparing Layered Silicates and Microcrystalline Cellulose as Nanoreinforcement *Composites Science and Technology* 66 2006: pp. 2187 – 2196.
20. **Kiziltas, A., Gardner, D. J., Han, Y., Yang, H-S.** Dynamic Mechanical Behavior and Thermal Properties of

Microcrystalline Cellulose (MCC)-filled Nylon 6 Composites *Thermochimica Acta* 519 2011: pp. 38 – 43. http://dx.doi.org/10.1016/j.tca.2011.02.026

21. **Eldessouki, M., Buschle-Diller, G., Gowayed, Y.** Poly(L-lysine)/Microcrystalline Cellulose Biocomposites for Porous Scaffolds *Polymer Composite* 32 (12) 2011: pp. 1937 – 1944.
22. **Abzalbekuly, B., Drumstaitė, L., Jankauskaitė, V., Fataraitė, E., Dzhanachmetov, O.** Influence of Filler Type on Polydimethylsiloxane Properties *Polymer Chemistry and Technology: Proceedings of Scientific Conference Chemistry and Chemical Technology*, Kaunas: Technologija, 2012: pp. 62 – 66.
23. **Althues, H., Henle, J., Kaskel, S.** Functional Inorganic Nanofillers for Transparent Polymers *Chemical Society Reviews* 36 2007: pp. 1454 – 1465.
24. **Denver, H., Heiman, T., Martin, E., Gupta, A., Borca-Tasciuc, D.-A.** Fabrication of Polydimethylsiloxane Composites with Nickel Nanoparticle and Nanowire Fillers and Study of Their Mechanical and Magnetic Properties *Journal of Applied Physics* 106 2009: p. 064909 (5 pages).
25. **Ferrando, R., Jellinek, J., Johnston, R. L.** Nanoalloys: From Theory to Applications of Alloy Clusters and Nanoparticles *Chemical Reviews* 108 (3) 2008: pp. 845 – 910.
26. **Guzmįn, M. G., Dille, J., Godet, S.** Synthesis of Silver Nanoparticles by Chemical Reduction Method and Their Antibacterial Activity *International Journal of Chemical and Biological Engineering* 2 (3) 2009: pp. 104 – 111.
27. **Hong, S., Lee, J. S., Ryu, J., Lee, S. H., Lee, D. Y., Kim, D. P., Park, C. B., Lee, H.** Bio-inspired Strategy for on-Surface Synthesis of Silver Nanoparticles for Metal/Organic Hybrid Nanomaterials and LDI-MS Substrates *Nanotechnology* 22 (49) 2011: p. 494020.
28. **Praus, P., Turicova, M., Machovič, V., Študentova, S., Klementova, M.** Characterization of Silver Nanoparticles Deposited on Montmorillonite *Applied Clay Science* 49 2011: pp. 341 – 345.
29. **Ferraria, A. M., et al.** Hybrid Systems of Silver Nanoparticles Generated on Cellulose Surfaces *Langmuir* 26 (3) 2010: pp 1996 – 2001.
30. **Drogat, N., Granet, R., Sol, V., Memmi, A., Saad, N., Koerkamp, C. K., Bressollier, P., Krausz, P. J.** Antimicrobial Silver Nanoparticles Generated on Cellulose Nanocrystals *Journal of Nanoparticle Research* 13 2011: pp. 1557 – 1562.
31. **Cao, H., Liu, X.** Silver Nanoparticle-Modified Films versus Biomedical Device-Associated Infections *Wiley Interdisci plinary Reviews. Nanomedicine and Nanobiotechnology* 2 (6) 2010: pp. 670 – 684. http://dx.doi.org/10.1002/wnan.113
32. **Thirumurugan, G., Dhanaraju, M. D.** Silver Nanoparticles: Real Antibacterial Bullets In: Antimicrobial Agents. V. Bobbarala (Ed.). InTech, 2012: pp. 407 – 422. http://dx.doi.org/10.5772/32450
33. **Rai, M., Yadav, A., Gade, A.** Silver Nanoparticles as a New Generation of Antimicrobials *Biotechnology Advances* 27 2009: pp. 76 – 78.
34. **Kheybari, S., Samadi, N., Hosseini, S.V., Fazeli, A., Fazeli, M. R.** Synthesis and Antimicrobial Effects of Silver Nanoparticles Produced by Chemical Reduction Method *DARU Journal of Pharmaceutical Sciences* 18 (3) 2010: pp. 168 – 172.
35. **Xiu, Z., Zhang, Q., Puppala, H. L., Colvin, V. I., Alvarez, P. J. J.** Negligible Particle-Specific Antibacterial Activity of Silver Nanoparticles *Nano Lett*ers 12 2012: pp.4271 – 4275.
36. Compendium of Methods for the Determination of Inorganic Compounds in Ambien Air. Compendium Method IO-3.2. Determination of Metals in Ambient Particulate Matter Using Atomic Absorption (AA) Spectroscopy. EPA/625/R-96/010a, 1999.
37. **Jucius, D., Grigaliūnas, V., Kopustinskas, V., Lazauskas, A., Guobiene, A.** Wettability and Optical Properties of O_2 and CF_4 Plasma Treated Biaxially Oriented Semicrystalline Poly(ethylene terephthalate) Films *Applied Surface Science* 263 (12) 2012: pp.722 – 729. http://dx.doi.org/10.1016/j.apsusc.2012.09.149
38. **Lazauskas, A., Grigaliūnas, V.** Float Glass Surface Preparation Methods for Improved Chromium Film Adhesive Bonding *Materials Science* (*Medžiagotyra*) 18 (2) 2012: pp. 181 – 186.
39. **Stalder, A. F., Kulik, G., Sage, D., Barbieri, L., Hoffmann, P.** A Snake-based Approach to Accurate Determination of Both Contact Points and Contact Angles *Colloids and Surfaces A: Physicochemical and Engineering Aspects* 286 (1 – 3) 2006: pp. 92 – 103.
40. Manual on Antimicrobial Susceptibility Testing. M.B Coyle, Ed. American Society of Microbiology, 2005: 236 p.
41. **Dehkordi, S. H., Hosseinpour, F., Kahrizangi, A. E.** An *in vitro* Evaluation of Antibacterial Effect of Silver Nanoparticles on Staphylococcus aureus Isolated from Bovine Subclinical Mastitis *African Journal of Biotechnology* 10 (52) 2011: pp. 10795 – 10797.
42. **Dror-Ehre, A., Mamane, H., Belenkova, T., Markovich, G., Adin, A.** Silver Nanoparticle-*E. coli* Colloidal Interaction in Water and Effect on *E. coli* Survival *Journal of Colloidal and Interface Science* 339 2009: pp. 521 – 526.
43. **Soo-Hwan, K., Lee, H.-S., Ryu, D.-S., Choi, S.-J., Lee, D.-S.** Antibacterial Activity of Silver-nanoparticles Against *Staphylococcus aureus* and *Escherichia coli* *Korean Journal of Microbiology and Biotechnology* 39 (1) 2011: pp. 77 – 85.